Original article

Sensory role of actin in auxin-dependent responses of tobacco BY-2

CrossMark

Xiang Huang*, Jan Maisch, Peter Nick

Botanical Institute, Karlsruhe Institute of Technology, Fritz-Haber-Weg. 4, Gbd. 30.43, (5. OG), 76131 Karlsruhe, Germany

ARTICLE INFO

ABSTRACT

Polar auxin transport depends on the polar localization of auxin-efflux carriers. The cycling of these carriers between cell interior and plasma membrane depends on actin. The dynamic of actin not only affects auxin transport, but also changes the auxin-responsiveness. To study the potential link between auxin responsiveness and actin dynamics, we investigated developmental responses of the non-transformed BY-2 (*Nicotiana tabacum* L. cv Bright Yellow 2) cell line and the transgenic BY-2 strain GF11 (stably transformed BY-2 cells with a GFP-fimbrin actin-binding domain 2 construct). The developmental process was divided into three distinct stages: cell cycling, cell elongation and file disintegration. Several phenotypes were measured to monitor the cellular responses to different concentrations of exogenous natural auxin (Indole-3-acetic acid, IAA). We found that auxin stimulated and prolonged the mitotic activity, and delayed the exit from the proliferation phase. However, both responses were suppressed in the GF11 line. At the stationary phase of the cultivation cycle, auxin strongly accelerated the cell file disintegration. Interestingly, it was not suppressed but progressed to a more complete disintegration in the GF11 line. During the cultivation cycle, we also followed the organization of actin in the GF11 line and did not detect any significant difference in actin organization from untreated control or exogenous IAA treatment. Therefore, our findings indicate that the specific differences observed in the GF11 line must be linked with a function of actin that is not structural. It means that there is a sensory role of actin for auxin signaling.

1. Introduction

Any living cell relies on internal and the external information to organize in time and space. For instance, a more or less symmetric zygote can divide and generate an embryo with clear axis and polarity, which will then develop into an independent and complex organism. This is only possible, because signals from the environment or the neighboring cells orient subcellular architecture of the cell as the basic structural and functional unit of development. This means that some components of subcellular architecture must be able to perceive and process orienting signals, and to transduce them into a morphogenetic response. For animal cells, the cytoskeleton, actin filaments and microtubules, is central for this signal-dependent morphogenetic response.

However, changes of cellular organization cannot only occur as response to signals, but might also be part of signaling itself. For instance, in mammalian cells, the glucocorticoid receptor will, upon binding of glucocorticoid ligands, translocate into the nucleus to regulate the transcription of specific genes (Rhen and Cidlowski, 2005). Likewise, in plant cells, red light can control gene expression by the photoreceptor phytochrome, which, upon irradiation, will shift into the nucleus and activate there the transcriptional regulator Phytochrome-Interacting Factor (Leivar and Quail, 2011).

The bidirectional relationship between signaling and cellular organization is reflected in a dual role of the cytoskeleton as central element of cytoplasmic architecture: The main role of the cytoskeleton in animal cells is to control cell shape. Since the cytoskeleton consists of elements able to confer compression forces (microtubules), and of elements able to confer traction forces (actin filaments), it can act as tensegral structure integrating mechanic forces over the entire cell. Whereas cytoskeletal tensegrity of animal cells is used to maintain cellular structure (Ingber, 2003), the situation is different in plant cells, where the architectural functions of the cytoskeleton are partially adopted by the plant cell wall, providing the potential for a functional shift of the cytoskeleton. Here, cytoskeletal tensegrity might be used for sensing or signal processing (Nick, 2013).

Several environmental signals, such as osmotic stress, cold and heat, act by exerting a mechanical force upon the plasma membrane (Los and Murata, 2004). Only in a second step, these mechanical forces are

translated into biochemical signals, which in walled plant cells involve the cytoskeleton–plasma membrane–cell wall continuum (Wyatt and Carpita, 1993; Pont-Lezica et al., 1993; Baluška et al., 2003). This functional unit has also been demonstrated for tobacco BY-2 cells (Gens et al., 2000), and is thought to perceive, integrate and process mechanical stimuli, and transduce them into appropriate responses of growth. These morphogenetic responses seem to be linked with cortical microtubules that establish and reinforce the axis of cell division and cell expansion by guiding the direction of cellulose deposition (Li et al., 2015). In addition to morphogenetic responses, external stimuli can cause other developmental responses of the target cells that are rather linked with the second component of the plant cytoskeleton, actin filaments. The importance of actin remodeling for programmed cell death is well established (Gourlay and Ayscough, 2005; Smertenko and Franklin-Tong, 2011). When actin filaments rapidly detach from the cell membrane and contract into dense cables, this is often a hallmark for ensuing cell death (Guan et al., 2013; Chang et al., 2015).

Developmental reorganization of actin seems to be linked with auxin. However, this response depends on organ and concentration – while IAA stimulates growth in coleoptiles linked with actin being organized in form of fine strands (rice: Wang and Nick, 1998; Holweg et al., 2004; Nick et al., 2009; maize: Waller et al., 2002), it inhibits growth in roots correlated with bundling of actin (Rahman et al., 2007). The reason for this apparent discrepancy has to be seen in the differential auxin sensitivity and the bell-shaped dose-response curve for auxin-dependent responses: Roots are more sensitive to auxin with the endogenous levels of auxin already being beyond the optimum, such that even relatively low concentrations of exogenous auxin inhibit root growth (Foster et al., 1952, 1955). In contrast, shoots and coleoptiles are less sensitive, such that exogenous auxin is stimulating growth. In fact, when the concentrations are raised progressively in maize coleoptiles beyond the optimum of growth, actin is bundled as well which and actin is repartitioned from a soluble into a sedimentable state (Waller et al., 2002).

On the other hand, polar auxin transport depends on the polar localization of auxin-efflux carriers (Robert and Friml, 2009). The cycling of these carriers between cell interior and plasma membrane depends on actin (Zhu and Geisler, 2015). Actin, in turn, is remodeled depending on auxin constituting a self-referring feedback loop that can act as oscillatory signaling hub (Nick, 2010).

This actin-auxin oscillator involves auxin-dependent recruitment of actin-associated proteins such as actin depolymerization factor 2 (Durst et al., 2013), but also integrates stress-related signals, such as superoxide ions generated by the membrane located NADPH oxidase RboH (Chang et al., 2015). Auxin employs these superoxide anions to trigger signaling across the membrane signals, involving activation of phospholipase D producing phosphatidic acid (PA) and phosphatidylinositol 4,5-bisphosphate (PIP$_2$). Since PA sequesters actin-capping proteins, and PIP2 the actin-depolymerization factor, exogenous auxin will modulate actin dynamics and bundling (Eggenberger et al., 2017). Among other implications, this actin-auxin oscillator model predicts that even slight changes of actin dynamics should alter the cellular responses to auxin. There are some indications supporting this prediction: Actin marker lines of Arabidopsis expressing the actin marker actin-binding domain of plant fimbrin (FABD2-GFP) showed a significant reduction in auxin transport (Holweg, 2007), and the auxin-dependent regeneration of tobacco protoplasts was affected leading to a high frequency of cells with an aberrant additional polarity (Zaban et al., 2013).

In the current study, we wanted to test, whether developmental responses to auxin are dependent on actin dynamics in walled cells as well. Although developmental responses of suspension cells are limited to cell proliferation, cell expansion, and synchronization into pluricellular chains, this developmental sequence is clearly under control of auxin in a very specific manner (Campanoni and Nick, 2005). One specific aspect of these auxin responses is a pronounced bell-shaped

dose-response curve, i.e. at high ($> 10\,\mu M$) concentrations, the response is less pronounced than for a lower ($1–2\,\mu M$) level of auxins (Foster et al., 1955). This is classically interpreted as manifestation of a two-point attachment towards a receptor (Foster et al., 1952). Therefore, it is important to include also such high concentrations, although they exceed the endogenous level of auxin by an order of magnitude. To address the potential link between auxin-responsiveness and actin dynamics, we used the transgenic line GF11, stably expressing the actin binding domain 2 of plant fimbrin in fusion with GFP (Sano et al., 2005). This domain is used as state-of-the art marker for plant actin, but also causes a slight, but significant decrease of actin dynamicity (Holweg, 2007; Zaban et al., 2013). We used the approach to phenotype the responses of this line to different concentrations of exogenous natural auxin, indole acetic acid, in comparison to the non-transformed BY-2 wild type. This cell strain has been extensively used for biochemical and cell-cycle studies for its strong proliferation activity (Nagata et al., 1992), where conditions (such as inoculation density) have been adjusted for maximal proliferation, such that other responses of this cell line are masked. However, this cell strain can release a residual developmental programme of a pith-parenchymatic cell, when cultivated appropriately (reviewed in Opatrný et al., 2014). We find specific differences that can be partially assigned to structural functions of actin (such as the role of actin for nuclear migration). However, we also can demonstrate reduced auxin sensitivity in GF11 and conclude from this a role of actin for auxin signaling.

2. Materials and methods

2.1. Cell cultivation

BY-2 (*Nicotiana tabacum* L. cv Bright Yellow 2) suspension cell lines (Nagata et al., 1992) were cultivated in liquid medium containing 4.3 g/L Murashige and Skoog salts (Duchefa, http://www.duchefa.com), 30 g/L sucrose, 200 mg/L KH$_2$PO$_4$, 100 mg/L inositol, 1 mg/L thiamine, and 0.2 mg/L (0.9 μM) of 2,4-dichlorophenoxyacetic acid (2,4-D), adjusted to pH 5.8. The cells were subcultivated weekly, inoculating 1.0–1.5 mL of stationary cells into fresh medium (30 mL) in 100-mL Erlenmeyer flasks corresponding to 10^5 cells·mL^{-1}. Preparatory studies had shown that the progression of the different developmental stages was dependent on the initial density of the culture. The cells were incubated at 26 °C under constant shaking on a KS260 basic orbital shaker (IKA Labortechnik, http://www.ika.de) at 150 rpm. Every three weeks, the stock BY-2 calli were subcultured on media solidified with 0.8% (w/v) agar (Roth, http://www.carlroth.com). Cells and calli of the transgenic BY-2 strain GF11, stably transformed BY-2 cells with a GFP-fimbrin actin-binding domain 2 (GFP-FABD2) construct (Sano et al., 2005), were cultivated on the same media as nontransformed wild-type cultures (BY-2 WT), but supplemented with 30 mg/L Hygromycin. The GF11 cell strain was kindly provided by Prof. Dr. S. Hasezawa (Graduate School of Frontier Sciences, The University of Tokyo, Japan).

2.2. Auxin treatments

After inoculation of the cells, indole-3-acetic acid (IAA; Roth, Karlsruhe, Germany) was added directly to final concentrations of 2 μM, 8 μM, 16 μM or 32 μM (to probe for a potential bimodality of the dose-response relation), using filter-sterilized stocks of 5 mM, 20 mM, 40 mM or 80 mM IAA dissolved in 96% ethanol, respectively. The concentration of 2 μM for the (easily oxidized) IAA is physiologically equivalent to the 0.9 μM of the (very stable) 2,4-D used as complement in all experiments. A cell culture without any added IAA was used as control group. Preparatory experiments using solvent controls with corresponding concentrations of ethanol did not show any significant effects. The effects of IAA were tested only over the first culture cycle, i.e. the inoculum was always coming from cells that had been cultivated

under control conditions (i.e. in the absence of exogenous IAA). In all experiments, the same, basal level of 2,4-D (0.9 µM) were present, required to sustain proliferation activity. In a control experiment (Suppl. Fig. S3) targeted to detect a potential influence of 2,4-D on IAA-dependent responses, the cells were cultivated either in 32 µM of exogenous IAA alone (i.e. omitting any 2,4-D), in 32 µM of 2,4-D alone, or in a combination of 31.1 µM IAA and the usual basal level (0.9 µM) of 2,4-D.

2.3. Quantification of cell division and cell viability

To determine mitotic indices, 0.5 mL aliquots of cell suspension were collected daily from days 1 to 5 after inoculation and fixed in Carnoy fixative (3: 1 [v/v] 96% [v/v] ethanol: glacial acetic acid) complemented with 0.25% (v/v) Triton X-100, and then stained with 2′-(4-hydroxyphenyl)-5-(4-methyl-1-piperazinyl)-2,5′-bi(1H-benzimidazole) trihydrochloride (Hoechst 33258, Sigma-Aldrich), which was prepared as a 0.5 mg/mL filter-sterilized stock solution in distilled water and used at a final concentration of 1 µg/mL. Cells were viewed under an AxioImager Z.1 microscope (Zeiss, Jena) using the filter set 49 (excitation at 365 nm, beam splitter at 395 nm, and emission at 445 nm). Mitotic indices were calculated as the number of cells in mitosis divided by the total number of cells counted. The values reported are based on the observation of 1500 cells from three independent experiments.

To quantify cell viability, 0.5 mL aliquots of cell suspension were collected daily from days 1 to 5 after inoculation. Each sample was transferred into custom-made staining chambers (Nick et al., 2000) to remove the medium, and then the cells were incubated in 2.5% (w/v) Evans Blue for 3 min according to Gaff and Okong'O-Ogola (Gaff and Okong'O-Ogola, 1971). The Evans Blue was eliminated by washing twice with fresh medium. The frequency of the unstained (viable) cells was determined as well as the cell number per milliliter using a Fuchs-Rosenthal hematocytometer under bright-field illumination.

2.4. Estimation of doubling times

As first step, time courses of cell density were established over the proliferation phase of the culture, by collecting 0.5 mL aliquots of the cell suspension daily from day 0 till the day 3, when proliferation activity began to weaken, and counting cells using a Fuchs-Rosenthal hematocytometer. Based on these time courses for cell density and the assumption of first-order kinetics:

$$\frac{dn}{dt} = k \cdot n$$

with n number of cells, and k the time constant of exponential growth, the natural logarithm

$$\ln(n(t)) = \ln(n(t=0)) + kt$$

should follow a straight line with a slope of k that could be approximated by linear regression. From the estimated value of k, doubling time τ (= duration of the cell cycle) could be estimated as based on the equation:

$$\ln(2 \cdot n(t=0)) = \ln(n(t=0)) + k\tau$$

as

$$\tau = \ln(2)/k.$$

The correlation coefficients for this estimates were > 0.95 in most cases. The values reported are based on the observation of 1500 cells from three independent experimental series.

2.5. Microscopy and quantitative morphometry

To determine division synchrony, aliquots (0.5 mL) of cell suspension were collected daily from days 0 to 5 after inoculation and immediately viewed under an AxioImager Z.1 microscope (Zeiss, Jena) equipped with an ApoTome microscope slider for optical sectioning, and recorded by a cooled digital CCD camera (AxioCamMRm).

Differential interference contrast images were obtained by a digital imaging system (AxioVision; Zeiss, Jena) and frequency distributions over the number of cells per individual file were constructed using the MosaiX function. For each picture, the MosaiX function of the AxioVision software was used to cover a 4 × 4 mm area with 121 single pictures at an overlay of 10%. Images were processed and analyzed using the AxioVision software (Rel. 4.5; Zeiss). Each data point represents 1500 individual cell files, respectively collected from three independent experimental series. The results were tested for significance by a *t*-test at the 95% confidence level.

3. Results

3.1. BY-2 cells in suspension pass a sequence of three stages

In order to address the role of actin in the regulation of auxin-dependent cellular responses, we need a framework to describe and compare these responses on a quantitative level. During their cultivation cycle, BY-2 cells undergo an ordered developmental process that can be subdivided into three distinct stages: cell cycling, cell elongation and file disintegration (Fig. 1). After inoculation, cells enter a cycling phase. During this period, cells divide in a fast pace in several cycles giving rise to cell files composed of 6–8 cells. The first division (duration τ_1) is longer than the subsequent (usually two) divisions (durations τ_2 and τ_3). After a few days, cells exit from the cycling stage (t_{ex}), and begin to elongate. Soon after, at t_{dis}, the last stage of the culture cycle, file disintegration, initiates. Hereby, after cell expansion, the connection between some cells in the same cell file becomes loose, and the cell file is divided into two shorter files. These smaller cell files decay further, until only unicellular and bicellular files are left at the end of the cultivation cycle. It should be noted that not all files have reached the terminal unicellular state by the end of the cultivation cycle, but continue their decay after subcultivation, i.e. at a time when the singular cells already enter the next round of cycling. Thus, during the first day of the culture cycle, a transition from a unicellular to a bicellular situation (by division, with a duration of τ_1), and a transition from incompletely disintegrated bicellular files into single cells (with a duration of τ_d) proceed in parallel. In the attempt to reach a more complete disintegration, we had also tested subcultivation intervals beyond 7 days. However, after day 7, viability dropped rapidly and drastically (data not shown), such that this approach was not meaningful. It should be mentioned that the progression and completeness of the developmental pattern described above was dependent on the initial density of the culture. When the inoculum was chosen higher than the 10^5 cells mL^{-1} used here, the lag phase between subcultivation and onset of proliferation was shortened, the exit from proliferation was delayed, and the disintegration of files at the end of the culture cycle was incomplete. On the other hand, when cell density was too low, this resulted in a prolonged lag phase and reduced proliferation.

3.2. The progression of mitotic activity is modulated by natural auxin (IAA)

We followed the mitotic index (MI) over time in the non-transformed BY-2 cell line (WT) and the transformed GF11 actin-marker line to define the temporal pattern of cell division. In the absence of exogenous IAA, mitotic index in the WT increased progressively reaching a peak at day 3 with almost 4% of cells encountered in mitosis, followed by a sharp decline to less than 1% at day 5 (Fig. 2A). In contrast, the mitotic index in the transgenic GF11 line was already high from day 1 and persisted at this level till day 3, when it declined in the same way as in the WT (Fig. 2A).

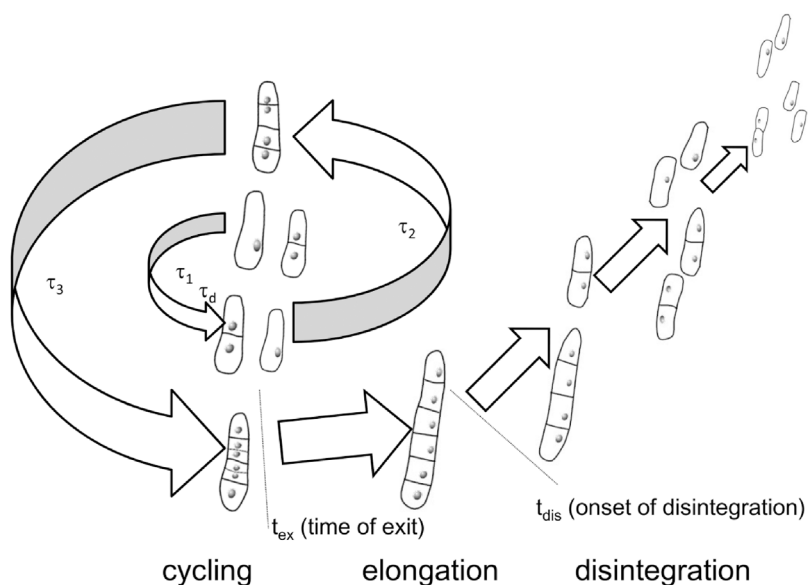This temporal pattern was modulated by IAA in a dose-dependent

Fig. 1. Schematic representation of the cultivation cycle and the parameters used for its quantitative description. The cycle is divided into three stages: cell cycling, cell elongation and cell disintegration with τ_1, τ_2 and τ_3 representing the duration of the first, second and third cell cycle, respectively, and τ_d the time constant for the decay of files that are still bicellular at subcultivation. The transition from cycling to elongation is described by t_{ex}, the onset of file disintegration by t_{dis}.

manner: The presence of IAA (2 μM) prolonged the rise of MI in the wild type by one additional day, such that a (higher) maximum of almost 5% was reached at day 4 (Fig. 2B). Again, this was followed by a sharp decline, but even at day 5, MI was significantly higher as compared to the untreated control (Fig. 2A). For GF11, 2 μM of IAA was not promoting mitotic activity, but in contrast caused a slight, but significant reduction, if compared to the situation without IAA (compare Fig. 2A and B). As a consequence, mitotic index in the transgenic line was consistently lower compared to the wild type, and did also not increase over time, but dropped sharply from day 4 (i.e. from the same time point, when also MI in the WT declined). Treatment with medium concentrations of IAA (8 μM and 16 μM) produced the same pattern as 2 μM (data not shown). However, for a high concentration of IAA (32 μM, included to test, whether the dose-response was bell-shaped), the MI for the WT was persistently at 3.5% between days 1 and 3 (Fig. 2C), which is close to the peak activity reached in the IAA-free control at day 3 (Fig. 2A). Instead, the decline after day 3 was very mild − at day 5, still 3% of the cells were found in mitosis (Fig. 2C), compared to less than 1% in the experiment without exogenous IAA (Fig. 2A). Under this high concentration of IAA, the transgenic GF11 behaved almost identically as the WT. The only difference was a significantly stronger decline of mitotic index following day 3 compared to the WT (Fig. 2C). It should be noted that the peak of the MI was now again at day 3 (as in the IAA-free control), and not at day 4 (as in the experiment with 2 μM of IAA). It should be mentioned that a basal level of 2,4-D (0.9 μM) was present in all experiments – this was required to sustain a stable level of cell proliferation.

In order to understand these effects of IAA on actin, we followed the organization of actin in the GF11 line through the culture cycle from day 1 through day 5 on a daily basis, either in untreated controls or in cells cultivated in presence of 2 μM or 32 μM IAA, respectively. We were not able to detect any disruption of the actin filaments for any of these treatments (Supplemental Fig. S1).

3.3. Auxin and actin increase doubling times in a synergistic manner

The duration of the plant cell cycle is under control of phytohormonal signals, and we therefore addressed the effect of auxin on doubling times in both cell lines based on time courses of cell density. We found that in both, WT and the GFP-FABD2 overexpressor GF11, doubling was slow immediately after subcultivation, but then accelerated to around 20–25 h per cycle (Fig. 3). For both lines, cell cycle duration was almost identical, and remained unchanged in presence of

2 μM IAA. Interestingly, a qualitative difference was observed for high auxin (32 μM IAA, roughly ten times above the typical endogenous levels). Here, the cell cycle became extremely slow in GF11 during day 1 (Fig. 3B), whereas in the WT there was no change compared to the auxin-free control (Fig. 3A). For the subsequent days, this initial difference vanished completely − for these later time points, the doubling time in GF11 was the same as in the WT and it was also the same as without auxin. This means that high auxin and overexpression of the GFP-FABD2 marker acted synergistically in slowing down the first cell division, but did not show such a synergy for the subsequent days.

3.4. File disintegration is delayed by auxin depending on actin

Cell division leads to pluricellular files that disintegrate into smaller units during the later phase of the cultivation cycle. To investigate the influence of auxin on the formation and disintegration of these supracellular structures, we constructed frequency distributions over number of cells per file, and determined the mean cell number per file to monitor the temporal pattern of file formation and decay in response to different concentrations of IAA. As long as the build-up of files by cell cycling is stronger than the decay of files, the mean value should increase reaching a maximum, when both processes are in balance, and it should decrease again, when file decay exceeds cell division in the non-decaying files. Under control conditions, in the absence of supplementary IAA, we found that the maximum value was reached one day earlier in the WT as compared to GF11 (Fig. 4A). When we added 2 μM (Fig. 4B) or 32 μM (Fig. 4C) IAA, it did not change the timing of this peak in GF11. Only the amplitude was decreased slightly, but not significantly. In contrast, in the wild type, the peak was delayed by one day for 2 μM of IAA (Fig. 4B), and for 32 μM of IAA this delay was accompanied by a significant increase of amplitude (Fig. 4C). It should be noted that the maximum file length was reached at a time point, when mitotic index was still increasing (compare Figs. 2 and 4). This means that disintegration of cell files initiates at a time point, when cells are still cycling. In the WT, auxin delays the onset of disintegration in parallel to prolonging the cycling stage of the culture. In the GF11 line, auxin cannot induce such a delay of disintegration (Fig. 4C), and it also does not prolong the cycling stage of the culture (Fig. 2C).

To get insight into the role of actin stabilization for responses that depend on polar auxin transport, we constructed frequency distributions over cell number per file over the cultivation cycle for both cell strains and for different concentrations of exogenous IAA. The third cell cycle in a file (leading to the transition from n = 4 to either n = 5 in
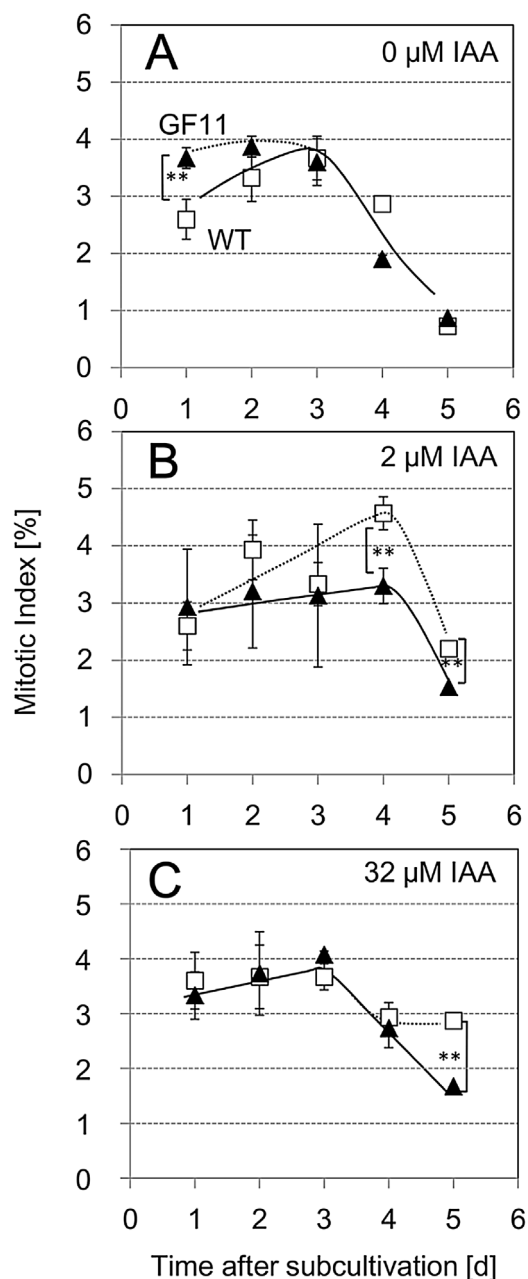
Fig. 2. Mitotic index of the non-transformed BY-2 cell line (WT, white squares) and the GFP-FABD2 overexpressor (GF11, black triangles) over time after subcultivation in the absence of (A), or in presence of 2 µM (B), or 32 µM (C) IAA. Each point is based on 1500 individual cells from three independent experimental series. Error bars indicate SE of the mean. Asterisks represent statistically significant differences (Student's *t*-test) with *P* < 0.01.
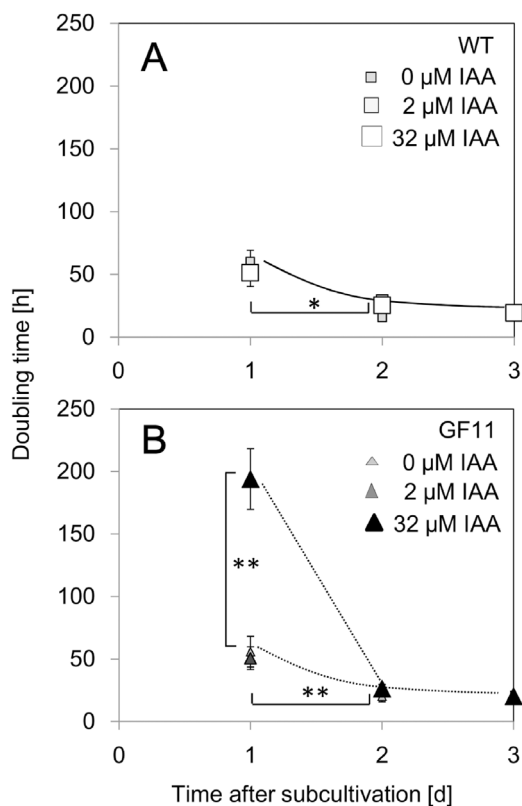

Fig. 3. Doubling time in the non-transformed BY-2 cell line (WT, A) and the GFP-FABD2 overexpressor (GF11, B) over time after subcultivation in the absence of IAA or in presence of 2 or 32 µM IAA, respectively. Each point is based on three independent experimental series. Error bars indicate SE of the mean. Asterisks represent statistically significant differences (Student's *t*-test) with *P* < 0.05 (*) and *P* < 0.01 (**), respectively.

case of asynchrony or to n = 6 in case of synchrony) depends on polar auxin transport (Campanoni et al., 2003; Maisch and Nick, 2007). We found that the GF11 line showed a priori a significant reduction of this synchrony (Supplemental Fig. S2), and this low synchrony did not significantly change when the concentration of exogenous IAA was raised over 2 µM, 8 µM, 16 µM till 32 µM. In contrast, the synchrony in the wild type dropped with increasing IAA concentration till it was as low as in GF11.

To address a potential influence of the basal level (0.9 µM) of the non-transportable artificial auxin 2,4-D, a supplementary experiment was conducted (Supplementary Fig. S3). In this experiment, WT BY-2 cells were cultivated either in 32 µM IAA (without 2,4-D), in a combination of 31.1 µM IAA with the usual basal level (0.9 µM) of 2,4-D, or

with 32 µM 2,4-D alone, i.e. in the absence of exogenous IAA. Then, the frequencies of cell number per file were determined at day 2 after subcultivation. The distribution patterns between IAA alone and the combination of low 2,4-D and IAA were almost identical (Suppl. Fig. S3). The only difference was a slightly (but significantly) reduced frequency of bicellular files in the absence of 2,4-D. In contrast, cells that had been exclusively treated with 32 µM 2,4-D, showed a conspicuous increase in the proportion of bicellular files, while the proportion of quadricellular file was strongly decreased as compared to the situation with 0.9 µM of 2,4-D and 31.1 µM IAA given in combination. These data show that the pattern of division synchrony is almost exclusively controlled by IAA, while 2,4-D only plays a very marginal role.

3.5. Auxin delays the exit from the cycling stage

At the late stage of cell cultivation, cell cycling activity weakens progressively, and file disintegration becomes dominant (see Fig. 1). When the time course of mitotic index (Fig. 2) is compared with the time course of mean cell number per file (Fig. 4), it becomes clear that file disintegration already initiated at a time, when cells still underwent mitotic cycling. To estimate the exit time from the cycling stage, we calculated the mitotic index data and set the maximal MI as 100%. Then we fitted a linear regression to the MI values of the following days. From the regression, we calculated the 50% value as exit point, i.e. the time, when 50% of the previously cycling population has stopped cycling. This exit point was delayed by around one day for 2 µM, 8 µM and 16 µM of IAA, as compared to the control (0 µM). Both WT and GFP-FABD2 overexpressor behaved identically with respect to this exit point (Fig. 5). However, for 32 µM of IAA, the cycling stage for the WT was strongly prolonged, which was not seen in the GF11. Thus, in analogy
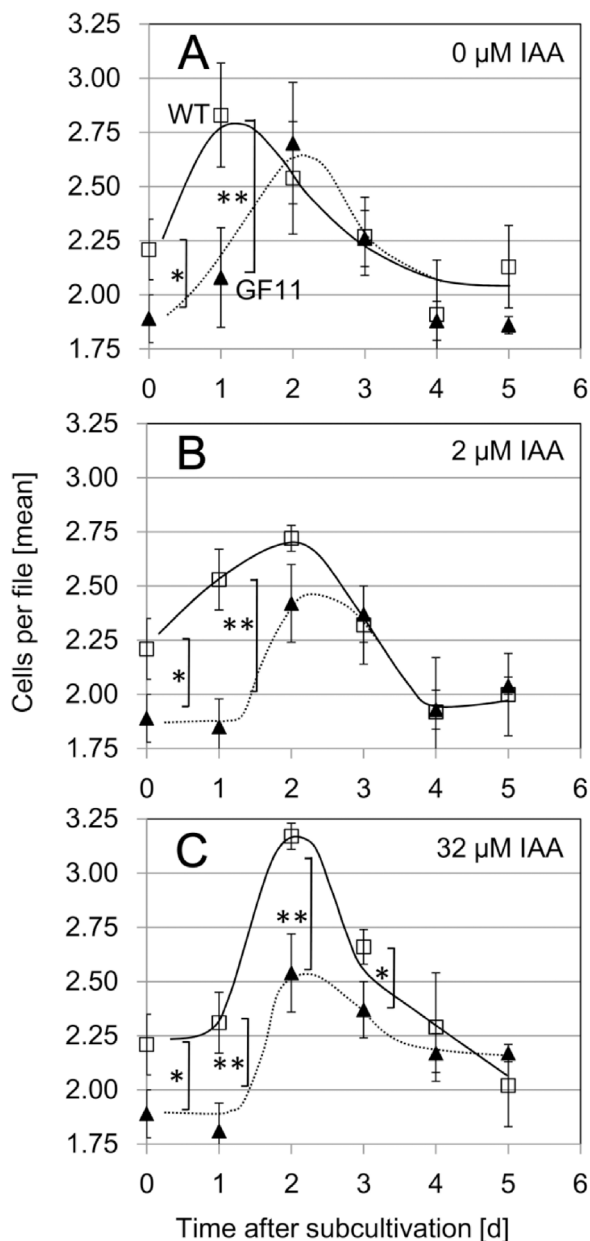
Fig. 5. Time of exit from the cycling stage in the WT (open squares) and the GFP-FABD2 overexpressor GF11 (black triangles) over the concentration of supplementary IAA. Each point is based on 1500 individual cells from three independent experimental series. Error bars indicate SE of the mean. Asterisks represent statistically significant differences (Student's t-test) with $P < 0.01$ (**).

Fig. 4. Mean cell number per file over time in the non-transformed BY-2 cell line (WT, open squares) and the GFP-FABD2 overexpressor (GF11, black triangles) over time after subcultivation in the absence of IAA (**A**), or in presence of 2 μM (**B**) or 32 μM (**C**) IAA. Each point is based on 1500 individual cell files from three independent experimental series. Error bars indicate SE of the mean. Asterisks represent statistically significant differences (Student's t-test) with $P < 0.05$ (*) and $P < 0.01$ (**), respectively.

with the delay of file disintegration, the response of exit from cycling to high levels of IAA seems to be suppressed in the GFP-FABD2 overexpressor line.

3.6. Auxin stimulates initial cell file decay depending on actin

In the whole population of BY-2 cells, not all the cells are synchronized. At the end of the cultivation cycle, there are still some cell files not reaching the terminal unicellular or bicellular files. After subcultivation, a new wave of vigorous cell division initiates (see Figs. 1 and 2). However, there is still a significant proportion (around 40%) of bicellular files that have not completely decayed to the unicellular stage. These bicellular files should produce a large frequency of quadricellular files during day 1 and 2. However, when we followed the
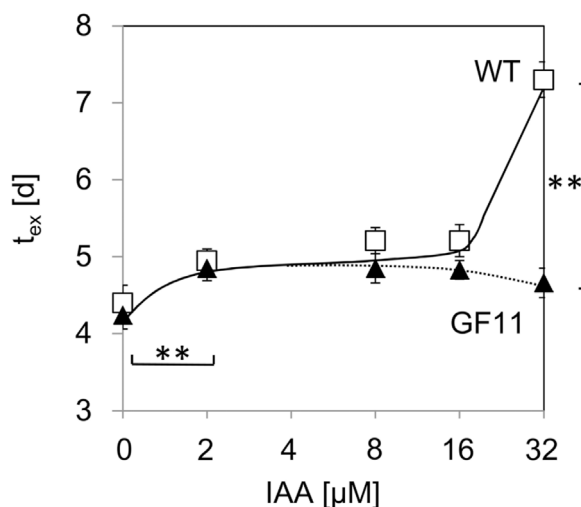
frequency distributions of cell number per file on a daily base time point after subcultivation, it turned out that there were high proportions of unicellular and bicellular files during days 0, 1 and 2 (data not shown). This means that most bicellular files must still undergo decay, whereas the completely disintegrated single cells already begin to enter a new cell cycle. If one neglects (the small frequency) files composed of more than two cells, it is possible to calculate the decay rates (bicellular to singular) for WT and GF11 over day 1. For the wild type in the absence of auxin, around 48 h were required to get from a bicellular to a unicellular situation (Fig. 6), but this was accelerated to around 24 h in presence of 2 μM or 32 μM IAA. This decay was considerably faster in the GFP-FABD2 overexpressor GF11. Here, in the absence of auxin, the rate was 18 h in absence of auxin and decreased to 6 h at 2 μM, and 4 h at 32 μM of IAA (Fig. 6). This means that auxin stimulates the decay of residual bicellular files and that this auxin response is accentuated in the GFP-FABD2 overexpressor. The fact that the time constant for the decrease of bicellular files is higher than that for doubling, also means that the vast majority of bicellular files first decays before entering a new cycle of mitosis.
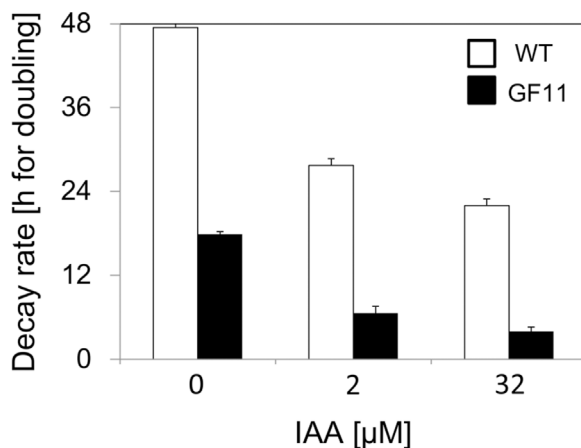

Fig. 6. Initial decay of cell files in the WT (white bars) and the GFP-FABD2 overexpressor GF11 (black bars) during day 1 after subcultivation in the absence of, or in presence of 2 μM or 32 μM IAA, respectively. Each point is based on 1500 individual cell files from three independent experimental series. Error bars indicate SE of the mean. Asterisks represent statistically significant differences (Student's t-test) with $P < 0.01$ (**).

4. Discussion

4.1. Cellular responses to auxin are modulated in the GFP-FABD2 overexpressor

To get insight into the role of actin for auxin-dependent developmental responses of walled plant cells, we mapped the behavior of tobacco BY-2 cells in the presence of different concentrations of the natural auxin (IAA) and compared the response patterns of the non-transformed line with a line overexpressing a GFP fusion of the actin-binding domain 2 of plant fimbrin. This actin marker confers a slight stabilization of actin (Holweg, 2007; Zaban et al., 2013), which, upon overexpression in *Arabidopsis thaliana*, can also cause subtle changes of growth, such as a reduced elongation of root hairs (Wang et al., 2008).

Using this marker, we have now addressed the effect of slight actin stabilization on the auxin responses in a tobacco suspension cell line by quantifying physiological readouts for actin-dependent responses. Since actin dynamicity can vary even between neighbouring cells within a cell file (Eggenberger et al., 2017), such a physiological approach is useful, because it integrates over the entire cell population. The use of cells in suspension to address such "developmental" aspects may be surprising at first sight. Suspension cell cultures are widely used as model for biochemical and cell biological studies, and the tobacco cell line BY-2 has acquired a certain celebrity in this respect as "HeLa cell line" of plant biologists (Nagata et al., 1992), because cell suspensions represent a convenient system to accumulate "biomass". However, their potential as systems to address cellular aspects of development has been rarely exploited. Although suspension cells are often designated as "dedifferentiated", they still preserve certain characteristics of their origin. In case of the BY-2 line, these characteristics include the reduced recapitulation of a developmental program seen in a pith parenchymatic cell that is stimulated by auxin to differentiate into a vascular bundle (Opatrný et al., 2014). Whereas this developmental sequence can even reach to the formation of secondary cell wall thickenings in other, slower, cell strains derived from pith parenchyma (Nick et al., 2000), the selection of BY-2 for rapid division has resulted in a cell strain that cannot sustain the viability of the auxin-depleted state long enough to develop these hallmarks of differentiation. Nevertheless, even in BY-2, there is a distinct and reproducible sequence of developmental stages including proliferation, formation of pluricellular files, transition to cell expansion, and progressive disintegration of the files into smaller units and eventually individual cells (Fig. 1). By stringent standardization of culture conditions, it is possible to reach a degree of reproducibility that allows us to deduce quantitative data from this system. Doing so, we were able to derive the following conclusions on the effect of auxin and actin stability:

Auxin stimulated and prolonged mitotic activity (Fig. 2), and delayed the exit from the proliferation phase (Fig. 5). Both responses were prominent for high concentrations of auxin, and both responses were suppressed in the FABD2 overexpressor line.

In contrast to these features, the length of the cell cycle, as monitored by the doubling times, was generally independent of auxin and actin (Fig. 3). However, the first cycle after subcultivation, which was considerably slower than the subsequent division cycles, was extremely retarded in the FABD2 overexpressor, but only in presence of high auxin concentrations.

Auxin not only delayed the exit from proliferation (Fig. 5), but also the disintegration of files exiting from the proliferation phase (Fig. 4). Both phenomena were suppressed in the FABD2 overexpressor. On the other hand, when acting on the residual bicellular files persisting at the end of the cultivation cycle, auxin strongly accelerated the disintegration of these residual files (Fig. 6). While it is difficult to directly observe, whether an incompletely decayed file already enters a new round of proliferation, it is possible to make a statistical statement: The time constant for the decrease of bicellular files was higher than that seen for proliferation. This means that the vast majority of bicellular

files first decays before entering a new cycle of mitosis, although it cannot be excluded that a small number of files already initiates a new cell cycle prior to complete disintegration of the file. In the FABD2 overexpressor, the disintegration was not only resistant to the retarding effect of auxin, but was generally progressing to a more complete disintegration in the later phase of the cultivation cycle, such that the incidence of bicellular files was significantly reduced. Furthermore, the auxin-dependent acceleration of disintegration was even stronger as compared to the non-transformed BY-2 wild type.

In summary, while some auxin responses were found to be retarded or downmodulated in the FABD2 overexpressors, others were seen to be either unaltered or even more pronounced. Interestingly, only few of these auxin responses followed a bell-shaped dose response, where the highest concentration (32 μM) was loosing activity if compared to the lower concentration (2 μM). This bimodal behavior is classically interpreted as manifestation of a receptor dimer (Foster et al., 1952, 1955). Interestingly, only the amplitude of mitotic index (Fig. 2) was following such a pattern, indicating that the activation of the cell cycle by auxin might differ from the activation of the other responses considered here.

It should be mentioned here that low concentrations (0.9 μM) of the non-transportable, artificial auxin (2,4-D) were added to probe for the function of transportable, natural auxin. This low background level of 2,4-D was required, because IAA is not completely stable over the entire cultivation cycle of 7 days. Over repeated cycles this degradation results in fluctuations of proliferation activity, which is avoided by 2,4-D. This non-transportable form of auxin has been shown to be inactive with respect to pattern formation and actin-dependent auxin transport (Maisch and Nick, 2007; Nick et al., 2009), but is required to sustain a stable basal level of proliferation (Campanoni and Nick, 2005). To probe for a potential influence of 2,4-D, we have compared the effect of a high (32 μM) concentration of exogenous auxins administered either completely in form of transportable IAA, of non-transportable 2,4-D, or a combination of a high (31.1 μM) concentration of IAA with the basal (0.9 μM) concentration of 2,4-D used in our experiments. Frequency distribution of cell number per file (as measure for division synchrony) was monitored as most sensitive readout (Suppl. Fig. S3). The data show clearly that division synchrony was accentuated by supplementary IAA, while presence or absence of 2,4-D was irrelevant. The fact that even in absence of exogenous IAA, a certain level of division synchrony was observed, indicates that 2,4-D activates the synthesis of endogenous IAA, a conclusion that had already been drawn earlier (Qiao et al., 2010) in experiments with a light-sensitive tobacco cell line.

To integrate these findings into a working model, in a first step, the observations will be grouped into phenomena seen at the onset of a new culture cycle, when stationary cells are confronted with exogenous IAA, and phenomena seen at the transition from the proliferation in the subsequent expansion phase of the culture.

4.2. At the onset of proliferation, FABD2 renders auxin responses more sensitive

At the end of the culture cycle, cells are highly vacuolated after several days of expansion growth. The nucleus is located at the periphery of the cell in a cytoplasmic pocket, from where transvacuolar strands of cytoplasm emanate. When a new cultivation cycle is initiated by transfer into fresh medium, the nucleus first has to migrate to the cell center, before the first division can initiate correlated with a significant increase of doubling time for the first division compared to the subsequent cycles that start from a situation, where the nucleus is already central (Fig. 3). Nuclear migration has been extensively studied in fungal systems and shown to depend on both, plus-end kinesin and minus-end dynein motors (Meyerzon et al., 2009; Fridolfsson and Starr, 2010). However, higher plants lack dynein motors − here, premitotic nuclear migration depends on so called kinesins with a calponin-homology domain (KCH), a plant-specific group of minus-end directed

class-XIV kinesins (Frey et al., 2010; Schneider and Persson, 2015). These kinesins exist in two functionally distinct subpopulations: either linked with actin filaments controlling premitotic nuclear movement, or uncoupled from actin in cell-wall related microtubule arrays, such as phragmoplast or cortical microtubules (Klotz and Nick, 2012). A link of nuclear migration with actin is not an exclusive acquisition of higher plants, but has also been observed in other organisms. For instance, actin-dependent tethering of the nucleus is a characteristic feature of cytoplasmic transport from nurse cells to the oocyte in the developing fruit fly follicle (Gutzeit, 1986). Moreover, several proteins responsible for the link between nuclear lamina and actin have been reported in mammalian cells (Razafsky and Hodzic, 2009). Although there is no nuclear lamina in plants, and although sequence homologues for some of these linker proteins seem to be absent, there exist functional analogues that convey the same function and link with plant-specific class-XI myosins (Tamura et al., 2013). The nuclear movement is associated with local contraction of a specific perinuclear actin basket at the leading edge indicating a peristaltic mechanism of movement (Durst et al., 2014). The extreme slow-down of the first cell cycle in response to 32 μM auxin was exclusively seen in the GFP-FABD2 overexpressor, indicating that the actin-dependent machinery driving nuclear movement is disrupted. When we followed potential structural changes of actin in response to IAA based on the GFP reporter (Supplemental Fig. S1), we were not able to detect any significant differences between control and IAA treatment. Specifically, there was no disruption of actin filaments to be seen. This indicates that the breakdown of nuclear movement caused by high concentrations of IAA in the GFP-FABD2 overexpressor is of functional, rather than of structural, nature. It should be mentioned here that the initial migration of the nucleus from the periphery towards the cell center requires that the cells have fully entered the expansion phase in the preceding cultivation cycle. This depends on the density in the inoculum – when the cells are cultivated at higher density, such that exit from proliferation is retarded and therefore the nucleus still not completely arrived at the cell periphery, this will mask the initial centripetal movement.

Not only was the nuclear movement at the initiation of a new culture cycle found to be sensitized against auxin upon overexpression of GFP-FABD2. Also the disintegration of the residual bicellular files had already progressed further in this cell strain, and this disintegration was further accelerated by exogenous auxin, and in the GFP-FABD2 strain, the amplitude of this acceleration was more pronounced (Fig. 6). This is remarkable, because file integrity depends on a different population of actin filaments that link neighboring cells through the plasmodesmata and are connected with a different class of plant specific class-VIII myosins that differ from the class-XI myosins involved in nuclear movement (Baluška et al., 2001).

Thus, at the onset of the proliferation phase, overexpression of GFP-FABD2 causes a sensitization of auxin responses.

4.3. At the progression of proliferation, FABD2 renders auxin responses less sensitive

The structural role of actin in the division of plant cells extends beyond steering and tethering the nucleus during its premitotic migration. It also extends over the role actin plays as a so called matrix that surrounds the division spindle (Forer and Wilson, 1994), and organizes the myosin-dependent cleavage of daughter cells (Mabuchi, 1986). In plant cells, actin filaments also participate in the control of division ability and symmetry: Once the nucleus has reached its final position, the transvacuolar actin cables fuse into a structure that spans the cell like a Maltesian cross oriented perpendicular to the long axis of the cell. While the microtubular preprophase band heralding axis and symmetry of the ensuing cell division is of transient nature and disappears in the very moment, when the nuclear envelope disintegrates, this so called actin phragmosome persists and lines a central zone, where actin is depleted (Sano et al., 2005; Nick, 2008). After the

separation of chromosomes, microtubules are organized into the interdigitating array of the phragmoplast and deliver vesicles containing cell wall material to the growing cell plate. The edge of the expanding cell plate is tethered to the zone of actin depletion, which had been previously occupied by the preprophase band. Thus, actin is considered to align the growth of the cell plate with the plane of symmetry (Kost and Chua, 2002). Exogenous auxin significantly stimulated mitotic activity and kept the cells in the proliferation phase, concomitantly with a delay of file disintegration (Figs. 4 and 5). Neither this delay, nor the stimulation of mitotic activity is seen in the GFP-FABD2 overexpressor, not even for the highest concentration of auxin (32 μM), indicating that, with progression into the proliferation phase, the responsiveness to auxin is reduced.

Thus, overexpression of GFP-FABD2 correlates with a desensitization of auxin responses (with progression into the proliferation phase), which is in sharp contrast seen to the increased sensitivity observed in stationary cells upon transition into the new culture cycle. What we show here, is nothing else than a sign-reversal with respect to the role of actin in auxin-dependent developmental responses. It is difficult to explain this sign-reversal by the structural functions of actin, since these structural functions (tethering of the nucleus via a process depending on class-XI myosins, symplastic continuity of neighboring cells via a process depending on class-VIII myosins) are similar. When we followed the GF11 line by spinning-disc microscopy over the culture cycle, we were not able to detect any significant difference in actin organization in response to different concentrations of exogenous IAA (Supplemental Fig. S1). This means that the specific differences observed in the GFP-FABD2 strain must be linked with a function of actin that is not structural.

4.4. A role for actin in auxin sensing

One candidate for such a role of actin that extends beyond the canonical structural effect of the cytoskeleton is the link between auxin transport and actin (Zhu and Geisler, 2015). Even the mild stabilization of actin filaments mediated by the overexpression of GFP-FABD2 in Arabidopsis can cause a substantial reduction in polar auxin transport (Holweg, 2007). Also for rice, actin stabilization caused by overexpression of mouse talin could be shown to impair auxin transport by using donor blocks of agar doped with radioactively labeled IAA and quantifying the proportion of radioactivity arriving in the receiver block (Nick et al., 2009). However, this approach is not feasible in suspension cells. The activity of polar auxin transport can be inferred by considering division synchrony across a cell file. Especially the synchrony of the third division is under control of polar auxin transport (Campanoni et al., 2003; Maisch and Nick, 2007). In case of asynchrony, a cell with n = 4 will move on to n = 5, in case of synchrony, a file with n = 6 will be produced. If the stabilization of actin by overexpression of GFP-FABD2 would impair the polarity of auxin transport, this should be seen as a significant reduction in the ratio of hexacellular over pentacellular files. This is exactly, what we have observed (Supplemental Fig. S2). By flooding the cell with extracellular IAA, the situation found in GF11 can be phenocopied in the wild type: in the presence of 32 μM IAA, the synchrony of the third division cycle has dropped to the value seen in the GFP-FABD2 overexpressor. Thus, a (mild) stabilization of actin, or likewise the out-competition of endogenous auxin gradients by an excess of exogenous IAA, reduce division synchrony in the same manner, indicative for a reduced polarity of auxin transport. This is consistent with previous work, where actin was destabilized by overexpression of actin-depolymerization factor 2 (ADF2) leading to disturbed division synchrony. Here, a mild stabilization of actin by low concentrations of phalloidin or by addition of phosphatidylinositol 4,5-bisphosphate (PIP$_2$) sequestering the excess ADF2 was able to rescue the division synchrony (Durst et al., 2013). Therefore, division synchrony requires that actin dynamics has to be balanced within a certain extent.

That the stabilization of actin should impair the polarity of auxin transport, would be expected from the actin-auxin oscillator model (Nick, 2010), since the stabilized actin filaments would trap the auxin efflux carriers, and thus interfere with their integration into the plasma membrane. Why the auxin-sensitivity of actin-dependent responses should undergo a sign-reversal, when cells pass on from stationary phase into a new cycle of proliferation, cannot be predicted by this model, though. Since these responses (for instance file disintegration) overlap with respect to the responsible actin arrays, explanations based on differently responsive actin subpopulations do not appear to be feasible either.

A simple way to explain sign-reversals in the response to a signal are mechanisms where this signal is perceived by two different receptors that switch their activity depending on the situation. In fact, tobacco cells have been shown to harbor two signaling chains that can be triggered by IAA. These chains differ with respect to functionality, perception and signaling (Campanoni and Nick, 2005): One signal chain is preferentially binding the artificial auxin 1-naphthalene acetic acid (NAA), is not sensitive to the G-protein inhibitor pertussis toxin, not activated by the G-protein activator aluminum tetrafluoride, and activates preferentially cell expansion. The other signal chain is preferentially binding the artificial auxin 2,4-D, is sensitive to pertussis toxin, activated by aluminum tetrafluoride, and activates preferentially cell division. There is also evidence for a differential interaction of these signaling chains with actin: treatment 2,3-butanedione monoxime (BDM), a generic inhibitor of myosins, not only causes a disorganization of cortical actin, but also delays the onset of cell division to auxin, while leaving cell expansion unaffected (Holweg et al., 2003). Moreover, different species of auxin differ in their ability to trigger a detachment of actin cables into fine filaments (Maisch and Nick, 2007; Nick et al., 2009): the natural auxin IAA, as well as its artificial analogue NAA are both transported in a polar manner are able to debundle actin. In contrast, 2,4-D, which only shows a poor polar transport, is also not effective in actin debundling.

The findings of the current study along with the concept of different auxin-signaling pathways can be integrated into the following working model (Fig. 7): In cells that have progressed into the proliferation phase, auxin activates a signal chain that activates the cell cycle and at the same time is linked with polar transport. This signaling requires dynamic actin and is therefore impaired, when actin is stabilized by overexpression of the GFP-FABD2 marker (auxin-actin oscillator, Fig. 7, left). If actin dynamics would drive a cycling of this receptor in a similar way as it does with the PIN proteins, bundling of actin should trap the receptor in a membrane-bound, intracellular and inactive state resulting in a desensitization of auxin signaling. In cells that have completed their proliferation phase, the cell-cycle related auxin signaling is expected to be down modulated, partitioning auxin signaling to cell expansion, dismantling of plasmodesmata-related actomyosin (leading to file disintegration), and nuclear migration to the cell periphery (Fig. 7, right). When this auxin signal chain competes with actin-dependent signaling for a common factor (common auxin signaling factor, Fig. 7, CAF) that is limiting, the desensitization of actin-dependent auxin signaling caused by the GFP-FABD2 marker might lead to a sensitization of this alternative actin-independent signaling chain.

This working model is admittedly speculative, but leads to clear predictions that can be tested in future experiments: since the auxin signal driving the cell cycle is dependent on actin dynamics as well, the GF11 line is expected to show a specific response to compounds that interfere with G-proteins, and it is also expected to produce different dose-response relations, if treated with NAA versus 2,4-D. Furthermore, if actin-dependent auxin signaling depends on the polar flux of auxin, inhibitors of auxin transport should not only cause a bundling of actin (Dhonukshe et al., 2008), but they should also reduce the sensitivity of the treated cell to exogenous auxin. Furthermore, direct subcellular localization of auxin using fluorescently labeled analogues (Hayashi et al., 2014) should allow deeper insight and therefore is already pursued in current experiments.
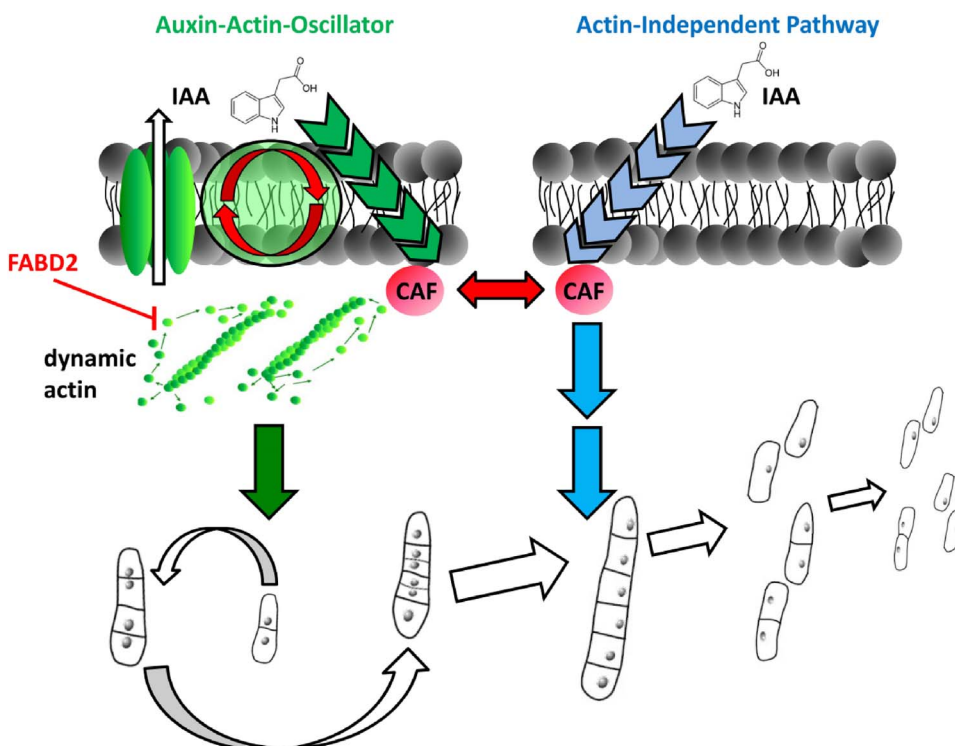
Acknowledgments

Fig. 7. Working model to explain the different actin-dependency of auxin responses in cycling versus stationary cells. The model is based upon the assumption of two different auxin signalling pathways. One pathway depends on dynamic actin and is active in proliferating cells (green) and is inhibited by overexpression of the fimbrin actin binding domain (FABD). Since dynamic actin also controls auxin efflux, an oscillatory circuit is established. The alternative pathway (blue) is active in stationary cells, is independent of actin dynamics and drives cell expansion, file disintegration, and nuclear positioning to the periphery. Auxin-actin oscillator and the actin independent auxin signalling compete for a common factor (operationally defined as common auxin signalling factor, CAF). As a consequence, activation of the actin-independent pathway by recruitment of the CAF will inhibit the auxin-actin oscillator.

Appendix A. Supplementary data

Supplementary data associated with this article can be found, in the online version, at http://dx.doi.org/10.1016/j.jplph.2017.07.011.

References

Baluška, F., Cvrčková, F., Kendrick-Jones, J., Volkmann, D., 2001. Sink plasmodesmata as gateways for phloem unloading. Myosin VIII and calreticulin as molecular determinants of sink strength? Plant Physiol. 126, 39–46.

Baluška, F., Šamaj, J., Wojtaszek, P., Volkmann, D., Menzel, D., 2003. Cytoskeleton-plasma membrane-cell wall continuum in plants: emerging links revisited. Plant Physiol. 133, 482–491.

Campanoni, P., Nick, P., 2005. Auxin-dependent cell division and cell elongation: NAA and 2,4-D activate different pathways. Plant Physiol. 137, 939–948.

Campanoni, P., Blasius, B., Nick, P., 2003. Auxin transport synchronizes the pattern of cell division in a tobacco cell line. Plant Physiol. 133, 1251–1260.

Chang, X., Riemann, M., Liu, Q., Nick, P., 2015. Actin as deathly switch? How auxin can suppress cell-death related defence. PLoS One 10, e0125498.

Dhonukshe, P., Grigoriev, I., Fischer, R., Tominaga, M., Robinson, D.G., Hašek, J., Paciorek, T., Petrášek, J., Seifertová, D., Tejos, R., Meisel, L.A., Zažímalová, E., Gadella, T.W.J., Stierhof, Y.D., Ueda, T., Oiwa, K., Akhmanova, A., Brocke, R., Spang, A., Friml, J., 2008. Auxin transport inhibitors impair vesicle motility and actin cytoskeleton dynamics in diverse eukaryotes. Proc. Natl. Acad. Sci. U. S. A. 105, 4489–4494.

Durst, S., Nick, P., Maisch, J., 2013. *Nicotianatabacum* actin-depolymerizing factor 2 is involved in actin-driven, auxin-dependent patterning. J. Plant Physiol. 170, 1057–1066.

Durst, S., Hedde, P.N., Brochhausen, L., Nick, P., Nienhaus, G.U., Maisch, J., 2014. Organization of perinuclear actin in live tobacco cells observed by PALM with optical sectioning. J. Plant Physiol. 141, 97–108.

Eggenberger, K., Sanyal, P., Hundt, S., Wadhwani, P., Ulrich, A.S., Nick, P., 2017. Challenge integrity: the cell-penetrating peptide BP100 interferes with the aux-in–actin oscillator. Plant Cell Physiol. 58 (1), 71–85.

Forer, A., Wilson, P.J., 1994. A model for chromosome movement during mitosis. Protoplasma 179, 95–105.

Foster, R.J., McRae, D.H., Bonner, J., 1952. Auxin induced growth inhibition a natural consequence of two point attachment. Proc. Natl. Acad. Sci. U. S. A. 38, 1012–1022.

Foster, R.J., McRae, D.H., Bonner, J., 1955. Auxin-antiauxin interaction at high auxin concentrations. Plant Physiol. 80, 323–327.

Frey, N., Klotz, J., Nick, P., 2010. A kinesin with calponin-homology domain is involved in premitotic nuclear migration. J. Exp. Bot. 61, 3423–3437.

Fridolfsson, H.N., Starr, D.A., 2010. Kinesin-1 and dynein at the nuclear envelope mediate the bidirectional migrations of nuclei. J. Cell. Biol. 191, 115–128.

Gaff, D.F., Okong'O-Ogola, O., 1971. The use of non-permeating pigments for testing the survival of cells. J. Exp. Bot. 22, 756–758.

Gens, J.S., Fujiki, M., Pickard, B.G., 2000. Arabinogalactan protein and wall-associated kinase in a plasmalemma reticulum with specialized vertices. Protoplasma 212, 115–134.

Gourlay, C.W., Ayscough, K.R., 2005. The actin cytoskeleton: a key regulator of apoptosis and ageing? Nat. Rev. Mol. Cell Biol. 6, 583–589.

Guan, X., Buchholz, G., Nick, P., 2013. The cytoskeleton is disrupted by the bacterial effector HrpZ, but not by the bacterial PAMP flg22 in tobacco BY-2 cells. J. Exp. Bot. 64, 1805–1816.

Gutzeit, H.O., 1986. The role of microfilaments in cytoplasmic streaming in *Drosophila* follicles. J. Cell Sci. 80, 159–169.

Hayashi, K.I., Nakamura, S.I., Fukunaga, S., Nishimura, T., Jenness, M.K., Murphy, A.S., Motose, H., Nozaki, H., Furutani, M., Aoyama, T., 2014. Auxin transport sites are visualized in planta using fluorescent auxin analogs. Proc. Natl. Acad. Sci. U. S. A. 111, 11557–11562.

Holweg, C., Honsel, A., Nick, P., 2003. A myosin inhibitor impairs auxin-induced cell division. Protoplasma 222, 193–204.

Holweg, C., Susslin, C., Nick, P., 2004. Capturing in vivo dynamics of the actin cytoskeleton stimulated by auxin or light. Plant Cell Physiol. 45, 855–863.

Holweg, C., 2007. Living markers for actin block myosin-dependent motility of plant organelles and auxin. Cell Motil. Cytoskelet. 64, 69–81.

Ingber, D.E., 2003. Tensegrity: II. How structural networks influence cellular information-processing networks. J. Cell Sci. 116, 1397–1408.

Klotz, J., Nick, P., 2012. A novel actin-microtubule cross-linking kinesin NtKCH, functions in cell expansion and division. New Phytol. 193, 576–589.

Kost, B., Chua, N.H., 2002. The plant cytoskeleton: vacuoles and cell walls make the difference. Cell 108, 9–12.

Leivar, P., Quail, P.H., 2011. PIFs: pivotal components in a cellular signaling hub. Trends Plant Sci. 16, 19–28.

Li, S.D., Lei, L., Yingling, Y.G., Gu, Y., 2015. Microtubules and cellulose biosynthesis: the emergence of new players. Curr. Opin. Plant Biol. 28, 76–82.

Los, D.A., Murata, N., 2004. Membrane fluidity and its roles in the perception of environmental signals. Biochim. Biophys. Acta 1666, 142–157.

Mabuchi, I., 1986. Biochemical aspects of cytokinesis. Int. Rev. Cytol. 101, 175–213.

Maisch, J., Nick, P., 2007. Actin is involved in auxin-dependent patterning. Plant Physiol. 143, 1695–1704.

Meyerzon, M., Fridolfsson, H.N., Ly, N., McNally, F.J., Starr, D.A., 2009. UNC-83 is a nuclear-specific cargo adaptor for kinesin-1-mediated nuclear migration. Development 136, 2725–2733.

Nagata, T., Nemoto, Y., Hasezawa, S., 1992. Tobacco BY-2 cell line as the Hela cell in the cell biology of higher plants. Int. Rev. Cytol. 132, 1–30.

Nick, P., Heuing, A., Ehmann, B., 2000. Plant chaperonins: a role in microtubule-dependent wall-formation? Protoplasma 211, 234–244.

Nick, P., Han, M., An, G., 2009. Auxin stimulates its own transport by actin reorganization. Plant Physiol. 151, 155–167.

Nick, P., 2008. Control of cell axis. Plant Cell Monogr. 143, 3–46.

Nick, P., 2010. Probing the actin-auxin oscillator. Plant Signal. Behav. 5, 94–98.

Nick, P., 2013. Microtubules, signalling and abiotic stress. Plant J. 75, 309–323.

Opatrný, Z., Nick, P., Petrášek, J., 2014. Plant cell strains in fundamental research and applications. Plant Cell Monogr. 22, 455–481.

Pont-Lezica, R.F., McNally, J.G., Pickard, B.G., 1993. Wall-to-membrane linkers in onion epidermis: some hypotheses. Plant Cell Environ. 16, 111–123.

Qiao, F., Chang, X.L., Nick, P., 2010. The cytoskeleton enhances gene expression in the response to the Harpin elicitor in grapevine. J. Exp. Bot. 61, 4021–4031.

Rahman, A., Bannigan, A., Sulaman, W., Pechter, P., Blancaflor, E.B., Baskin, T.I., 2007. Auxin, actin and growth of the *Arabidopsis thaliana* primary root. Plant J. 50, 514–528.

Razafsky, D., Hodzic, D., 2009. Bringing KASH under the SUN: the many faces of nucleo-cytoskeletal connections. J. Cell Biol. 186, 461–472.

Rhen, T., Cidlowski, J.A., 2005. Antiinflammatory action of glucocorticoids—new mechanisms for old drugs. N. Engl. J. Med. 353, 1711–1723.

Robert, H.S., Friml, J., 2009. Auxin and other signals on the move in plants. Nat. Chem. Biol. 5, 325–332.

Sano, T., Higaki, T., Oda, Y., Hayashi, T., Hasezawa, S., 2005. Appearance of actin microfilament 'twin peaks' in mitosis and their function in cell plate formation, as visualized in tobacco BY-2 cells expressing GFP-fimbrin. Plant J. 44, 595–605.

Schneider, R., Persson, S., 2015. Connecting two arrays: the emerging role of actin-microtubule cross-linking motor proteins. Front. Plant Sci. 6, 415.

Smertenko, A., Franklin-Tong, V.E., 2011. Organisation and regulation of the cytoskeleton in plant programmed cell death. Cell Death Differ. 18, 1263–1270.

Tamura, K., Iwabuchi, K., Fukao, Y., Kondo, M., Okamoto, K., Ueda, H., Nishimura, M., Hara-Nishimura, I., 2013. Myosin XI-i links the nuclear membrane to the cytoskeleton to control nuclear movement and shape in Arabidopsis. Curr. Biol. 23, 1776–1781.

Waller, F., Riemann, M., Nick, P., 2002. A role for actin-driven secretion in auxin-induced growth. Protoplasma 219, 72–81.

Wang, Q.Y., Nick, P., 1998. The auxin response of actin is altered in the rice mutant *Yin-Yang*. Protoplasma 204, 22–33.

Wang, Y.S., Yoo, C.M., Blancaflor, E.B., 2008. Improved imaging of actin filaments in transgenic Arabidopsis plants expressing a green fluorescent protein fusion to the C- and N-termini of the fimbrin actin-binding domain 2. New Phytol. 177, 525–536.

Wyatt, S.E., Carpita, N.C., 1993. The plant cytoskeleton −cell wall continuum. Trends Cell Biol. 3, 413–417.

Zaban, B., Maisch, J., Nick, P., 2013. Dynamic actin controls polarity induction de novo in protoplasts. J. Integr. Plant Biol. 55, 142–159.

Zhu, J.S., Geisler, M., 2015. Keeping it all together: auxin-actin crosstalk in plant development. J. Exp. Bot. 66, 4983–4998.